Applied Water Science (2020) 10:207
https://doi.org/10.1007/s13201-020-01282-4

ORIGINAL ARTICLE

Photocatalytic degradation of Rhodamine B dye with TiO_2 immobilized on SiC foam using full factorial design

Paul Henri Allé[1] · Guy Didier Fanou[1] · Didier Robert[2] · Kopoin Adouby[1] · Patrick Drogui[3]

Received: 21 January 2020 / Accepted: 21 July 2020

Abstract

Textile effluents treatment is one of the important environmental challenges nowadays. Photocatalysis has proven its effectiveness for the removal of recalcitrant compounds, and it is considered as a green technology for the treatment of effluents. However, good photocatalytic yield is strongly related to the operating parameters. In this study, a supported TiO_2 on a β-SiC foam was tested for the removal of Rhodamine B (RhB). The photocatalytic discoloration of RhB synthetic solution in our condition was about 90%. The effects of each parameter were assessed through a full factorial design. Sixteen tests were carried out and the response was RhB removal. The most influent parameters were TiO_2/β-SiC foam quantity, the concentration of RhB, the volume of H_2O_2 and pH. Their contributions on RhB removal were, respectively, 53.01, 30.49, 2.7, and 2.48% according to Pareto diagram. Analysis of the coefficients shows that initial concentration of RhB and volume of H_2O_2 had a negative effect on the response. However, the quantity of TiO_2/β-SiC foam and pH had a positive effect on the response. The influence of the flow rate on the process was assessed. The results showed a slight increase in RhB removal. Furthermore, the aging test of TiO_2/β-SiC foam on the photocatalytic efficiency was carried out after ten successive photocatalysis tests. Only 6.7% loss of yield was observed. These results are very encouraging for an application at the industrial scale.

Keywords Photocatalysis · TiO_2/β-SiC foam · Rhodamine B · Factorial design

Introduction

The agricultural and industrial sectors as well as household release each day a huge amount of pollutants into surface water, making them nonusable (Telegang 2017). Among them, the most well known are pharmaceutical products, phenolic compounds, and dyes (Bouyarmane 2014). Synthetic dyes are widely used in numerous industries such as textile, printing, food, cosmetic, clinical, paper, leather, pharmaceutical, and food industries (Martínez-Huitle and Brillas 2009). In fact, world production of dyes is estimated at 800,000 T/year and about 140,000 T/year is released in the environment during the fabrication and coloring steps of textiles (Mansour et al. 2011).

Dye effluent may contain chemicals that are toxic, carcinogenic, or mutagenic, to various fish species (Verma et al. 2012). It may also prevent light penetration in water and photosynthesis, which can drive to a lack of dissolved oxygen and upset the biological metabolism processes (Joshi et al. 2004; Assémian et al. 2018).

However, they can be removed by different processes: electrocoagulation (Assémian et al. 2018), Fenton (Briton

✉ Kopoin Adouby
adoubyk@yahoo.fr

Paul Henri Allé
paulhri33@gmail.com

Guy Didier Fanou
fanou_didier@hotmail.com

Didier Robert
didier.robert@univ-lorraine.fr

Patrick Drogui
patrick.drogui@ete.inrs.ca

[1] Laboratoire des Procédés Industriels de Synthèse, de l'Environnement et des Energies Nouvelles (LAPISEN), Institut National Polytechnique Félix Houphouët-Boigny, BP 1093, Yamoussoukro, Côte d'Ivoire

[2] Institut de Chimie de Procédé pour L'Energie, L'Environnement et la Santé (ICPEES-UMR 7515 CNRS), Université de Strasbourg, Strasbourg, France

[3] Institut National de la Recherche Scientifique (INRS Eau Terre et Environnement), Université du Québec, 490 rue de la Couronne, Quebec City, Canada

Published online: 17 August 2020

et al. 2018), coagulation/flocculation (Bouyakoub et al. 2010), adsorption using activated carbon, membrane filtration (Han et al. 2016; Sattar et al. 2017), and combined coagulation/carbon adsorption (Papić et al. 2004). Though these processes give good results, they have some drawbacks. Indeed, adsorption is selective and is just a transfer of pollutants from the aqueous phase to the solid one, and at bottom leads to another contamination. Fenton requires a lot of reagents, and electrocoagulation generates sludge at the end of the process. One way to destroy pollutants without using reagent and generating secondary toxic materials is photocatalysis (Asiri et al. 2011). Photocatalytic degradation, as a cheap and environmentally eco-friendly technology, has drawn extensive attention (Spasiano et al. 2015).

The type of photocatalyst used plays a key role in photocatalytic efficiency. TiO_2 has been investigated for the removal of hazardous compounds in water. Owing to its non-toxicity, low-cost, and good stability property compared to other materials (Ansari et al. 2016), TiO_2 is currently used in photocatalytic process. The effectiveness of this process on dyes removal has been widely demonstrated in many studies (Sacco et al. 2018; Yang and Yang 2018).

Besides, effectiveness of photocatalytic degradation is strongly related to the operating conditions such as TiO_2 concentration (powder), light intensity, pH, concentration of pollutants, and the presence of certain ions. Sometimes, the effectiveness of one parameter can be related to another one. Many publications have dealt with the degradation of dye using TiO_2 films (Wu and Zhang 2004; Crişan et al. 2018), TiO_2 nanocomposite (Hariprasad et al. 2013; Viet et al. 2018; Sanzone et al. 2018), and in suspension (Hafizah and Sopyan 2015). Among all of them, the best results were obtained with TiO_2 in suspension because it provides a better contact between TiO_2 and the pollutants. However, the use of TiO_2 powder causes the clogging of lamps and requires an expensive filtering process after the treatment. Hence, studies have been oriented on the immobilization of TiO_2 nanoparticles but the photocatalytic efficiencies are less than in suspension mode due to the reduction in the contacts between photocatalyst and pollutants. For this reason, β-SiC alveolar foam is a good support for the immobilization of the catalyst. Its three-dimensional structure improves the contact between the organic pollutant and the supported catalyst.

TiO_2/β-SiC foam material has proven its effectiveness for the removal of organic pollutants (Marien 2017; M'Bra et al. 2019). Parameters which are commonly studied in photocatalytic process are pH, dye concentration, mass of catalyst, and effect of electron acceptors such as H_2O_2, KB_rO_3, K_2SO_2, etc. (Aliabadi and Sagharigar 2011; Seck et al. 2012; Hamidi and Kacem 2017). To our knowledge, few studies have evaluated the effect of one parameter on another and the interaction between parameters on the removal process. Furthermore, the classical method which consists of varying one factor at a time and keeping others constant is not sufficient to explain the phenomenon entirely, and it is time-consuming. In this case, full factorial design is carried out to achieve the best optimization of the process (Elhalil et al. 2016). This design determines the effect of each factor on the response as well as the manner in which each factor varies with the change in the level of the other factors (Arenas et al. 2007). Interaction effects of different factors could be attained using experimental design (Montgomery 1997; Brasil et al. 2005). This technique is used to reduce the number of experiments, time, overall process cost. The objective of this study was to assess the interaction effects of each parameter and their effects on the photocatalytic performance using TiO_2/β-SiC foam.

Materials and methods

Materials

RhB dye was procured from Fluka, Germany (purity ≥ 99%), and its characteristics are mentioned in Table 1. Hydrogen peroxide (purity ≥ 95%), nitric acid (purity ≥ 99.5%), and sodium hydroxide (purity ≥ 95%) were provided by Panreac (Spain). All solutions were prepared with distilled water. Cylindrical-shape foam (35 mm diameter; 50 mm length) was provided by SICAT (German). The β-SiC foams were calcinated at 1000 °C for 2 h in order to remove the residual organic carbon. The deposition of TiO_2-P25 onto β-SiC foams was made by dip coating. Each foam was completely immersed in a suspension (10 g of TiO_2-P25 and 4 mL of TTIP in 200 mL of dry ethanol) for 3 min at 5 rpm. This

Table 1 Physicochemical properties of Rhodamine B

Properties	Values
Molecular structure	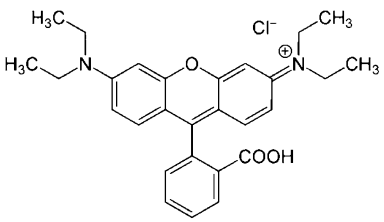
Chemical formula	$C_{28}H_{31}ClN_2O_3$
IUPAC name	Chloride of [9-(2-carboxyphenyl)-6-diethylamino-3-xanthenylidene]-diethylammonium
Molecular weight (g/mol)	479.02
pKa	50 (20 °C)
λ_{max} (nm)	554
Class	Cationic dye
Name (CI)	Basic Violet 10
Color index (CI) number	45170

process was repeated five times. Then, the photocatalytic materials were dried at room temperature for 20 min, avoiding clogging of the alveoli. Subsequently, TiO_2/β-SiC foams were placed in an oven at 110 °C overnight to evaporate residual organic compounds. After that, TiO_2/β-SiC foams were brought to the furnace at 450 °C for 2 h at a rise rate of 5 °C min^{-1}. The average weight of TiO_2 fixed on each foam is 1.5 g.

Photo-reactor and UV source

The photoreactor (Fig. 1) consisted of one coaxial quartz tube (400 mm length, ID 40 mm) placed inside a Pyrex glass cylinder. The quartz tube was filled with the TiO_2/β-SiC foam. TiO_2 (1.5 g) was coated on each foam giving a total mass of 10 g (foam + TiO_2). Four UV-A lamp tubes (Philips F8T5/BL) of 8 Watts with a maximum emission at approximately 365 nm were placed around the quartz tube and within the Pyrex glass cylinder. The total light intensity in the reactor was 14 W/m^2.

Experimental procedure

The working solutions were obtained by dilution of a stock solution of 100 ppm prepared by dissolving required mass of RhB dye in distilled water. Degradation tests were performed by circulating the RhB solution within 120 min through the photoreactor containing four TiO_2/β-SiC foams, using a peristaltic pump (MasterFlex, model 7520-47) at variable flow rate between 4 and 12 mL s^{-1}. pH was adjusted at a desired value before each test. One milliliter of the solution was extracted at regular time intervals to follow the kinetics of degradation. The residual concentration was determined with a JASCO UV–Vis spectrophotometer ($\lambda = 554$ nm).

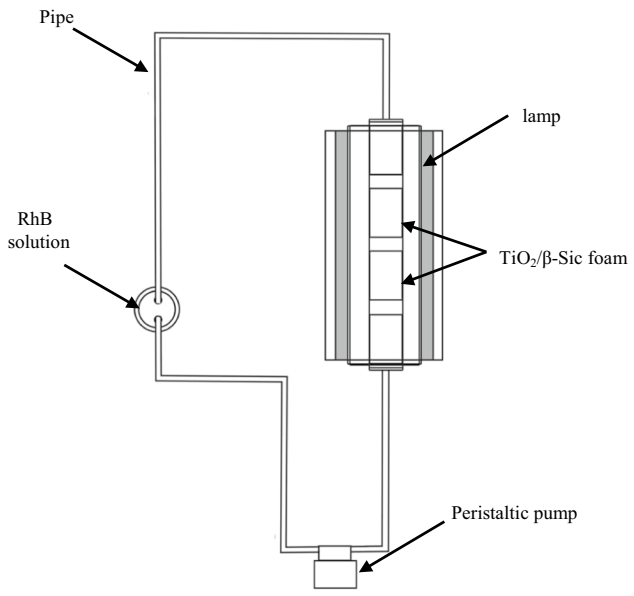

Fig. 1 Schematic representation of experimental setup

Experimental design

Two levels were chosen for each parameter, a higher level denoted (+) and a lower level denoted (−). In this study, a full factorial design (FFD) was used (2^4). It resulted in a combination of all levels of each factor (Assidjo et al. 2005). Thus, 16 experiments were carried out and the chosen parameters were pH (X_1), concentration of RhB (X_2), volume of H_2O_2 (X_3), and the number of TiO_2/β-SiC foam (X_4) (Table 2). The experimental domain is shown in Table 2. The response obtained was RhB removal rate (Y).

The RhB removal rate was calculated to according Eq. 1:

$$y_i = \frac{C_o - C_r}{C_o} \times 100 \quad (1)$$

C_0 is the initial RhB concentration and C_r is final RhB concentration.

In a full factorial design, the response studied is considered to be linear for all factors and can be represented by a linear polynomial function where b_0 represents the average response. b_i is the estimation of the principal effect of the factor i for the response Y and b_{ij} the interaction effect between factors i and j for the response Y investigated of RhB removal.

$$\begin{aligned} Y = {} & b_0 + b_1X_1 + b_2X_2 + b_3X_3 + b_4X_4 \\ & + b_{12}X_1X_2 + b_{13}X_1X_3 + b_{14}X_1X_4 + b_{23}X_2X_3 \\ & + b_{24}X_2X_4 + b_{34}X_3X_4 + b_{123}X_1X_2X_3 + b_{124}X_1X_2X_4 \\ & + b_{134}X_1X_3X_4 + b_{234}X_2X_3X_4 + b_{1234}X_1X_2X_3X_4 \end{aligned} \quad (2)$$

Table 2 Experimental domain for full factorial design

Factors	Values (X_i)	Experimental region	
		Low level (−1)	High level (+1)
pH	X_1	4	9
Concentration RhB (ppm)	X_2	10	30
Volume of H_2O_2 (mL)	X_3	1	3
Quantity of foams	X_4	2	4

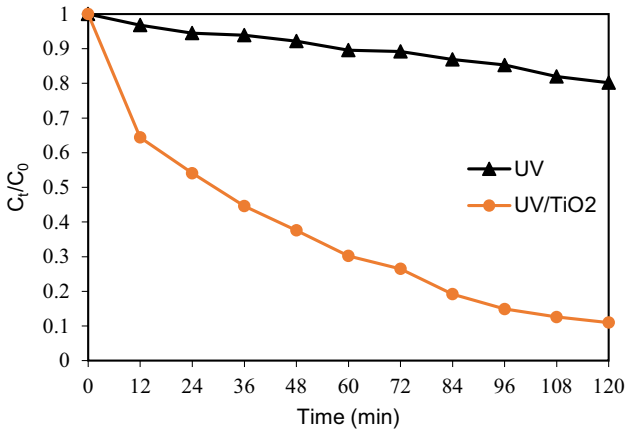

Fig. 2 Photocatalytic tests with TiO_2/β-SiC foam (C_{RhB} = 10 ppm, flow rate = 4 mL s^{-1}, T = 25 °C)

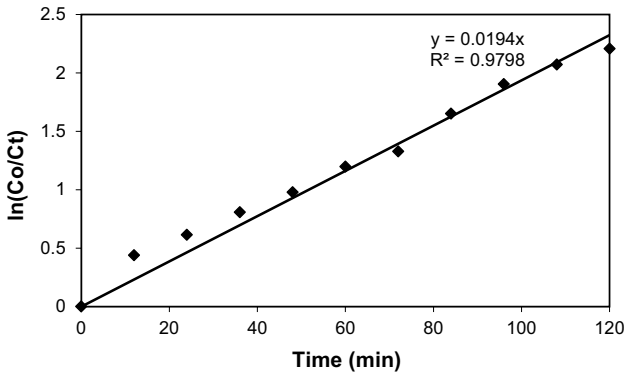

Fig. 3 Linearization from Langmuir–Hinshelwood model

Results and discussion

Comparison of photolysis and photocatalysis photocatalytic

Figure 2 shows both photolysis and photocatalysis results. The photolysis discoloration under UV radiation (365 nm) was weak, with only 20% of removal after 120 min. These results are different from the 90% removal obtained by Hamidi and Kacem (2017) using direct photolysis. This difference may be explained by the fact that they used in their study UVC (254 nm) which produces higher energy. This high photon energy ($h\nu$) facilitates the H_2O photolysis and the production of hydroxyl radicals according to Eq. 3:

$$H_2O + h\nu \rightarrow \cdot OH + H\cdot \quad (3)$$

However, in the photocatalytic reaction, RhB was almost fully removed. The discoloration was about 90%. Applying the Langmuir–Hinshelwood equation with solutions highly diluted, the reaction follows an apparent first-order kinetic. $\ln(C_0/C_r)$ versus time was linear line (Fig. 3) with R^2 of 0.979 and an apparent constant rate K_{ap} of 194.10^{-4} min^{-1}.

Modeling of the photocatalytic discoloration of RhB

Photocatalytic discoloration efficiency (Y) was measured for each factor, and the results are in Table 3. The predicted value (Y_{calc}) and the measured values were very close, which indicated a good correlation between the model and experimental results. The coefficients of the polynomial model were calculated using the NemrodW Software (Ano et al. 2019) as follows:

Table 3 Experimental design matrix and response based on the experimental runs and predicted values on discoloration of RhB

N°Exp	X_1	X_2	X_3	X_4	$Y_{exp.}$	$Y_{calc.}$	Difference
1	−1	−1	−1	−1	76.500	75.119	1.381
2	1	−1	−1	−1	78.500	80.699	−2.199
3	−1	1	−1	−1	52.700	53.926	−1.226
4	1	1	−1	−1	62.790	60.746	2.044
5	−1	−1	1	−1	62.600	63.486	−0.886
6	1	−1	1	−1	69.430	67.726	1.704
7	−1	1	1	−1	58.700	57.969	0.731
8	1	1	1	−1	61.900	63.449	−1.549
9	−1	−1	−1	1	94.660	94.489	0.171
10	1	−1	−1	1	97.260	96.614	0.646
11	−1	1	−1	1	71.800	72.126	−0.326
12	1	1	−1	1	75.000	75.491	−0.491
13	−1	−1	1	1	83.200	83.866	−0.666
14	1	−1	1	1	84.500	84.651	−0.151
15	−1	1	1	1	78.000	77.179	0.821
16	1	1	1	1	79.200	79.204	−0.004

Table 4 Value of model coefficient

Name	Coefficient	Signif. %
b_0	74.171	< 0.01***
b_1	1.901	1.38*
b_2	− 6.660	< 0.01***
b_3	− 1.980	1.18*
b_4	8.781	< 0.01***
b_{12}	0.310	57.1
b_{13}	− 0.335	54.2
b_{23}	3.919	0.0607***
b_{14}	− 0.864	15.2
b_{24}	− 0.292	59.3
b_{34}	0.252	64.3

The number of asterisks is related to the power of the coefficient; the more significant is the coefficient, the more number of asterisks it has; the number of asterisks ranges from 0 to 3; 0 means no significance of the coefficient

Main interactions

The coefficient $b_0 = 74.171$ represents the average value of the response of the 16 assays. Table 4 shows that RhB discoloration was highly positively influenced by foam quantity ($b_4 = 8.78$). RhB removal percentage increases on average 17.56 (2 × 8.78) when foam number was increased from 2 to 4. These results are similar to those of Al-Kahtani (2016) and Antoniou and Dionysiou (2007). They showed that the increase in TiO_2 quantity resulted in an increase in active sites on which OH– was oxidized to produce hydroxyl radicals which contribute to RhB removal. The second most important factor according to the Pareto diagram was pollutant's concentration which has a negative effect on the removal ($b_2 = -6.67$). The increase in RhB concentration induced a decrease in removal rate on average 13.34% (2 × 6.67), when concentration was increased from 10 to 30 ppm. This result can be explained by a decrease in the transmittance of the solution with the increase in the concentration of RhB, leading to fewer photons reaching the photocatalyst surface,

$$Y = 74.17 + 1.9X_1 - 6.66X_2 - 1.98X_3 + 8.78X_4 + 0.31X_1X_2 - 0.34X_1X_3 + 3.92X_2X_3 - 0.29X_2X_4 + 0.252X_3X_4 \quad (4)$$

Main and interaction effects were determined through experimental results (Table 4).

Using the Pareto diagram enables the calculation of the effect (%) of each factor on the response, according to Eq. 5 (García-Gómez et al. 2014):

$$p = \frac{b_i^2}{\sum b_i^2} \times 100 (i \neq 0) \quad (5)$$

Figure 4 shows that foam number was the most important factor (53.01%), next RhB initial concentration (30.49%). The most relevant interaction obtained was between initial concentration of RhB and H_2O_2 volume (10.56%).

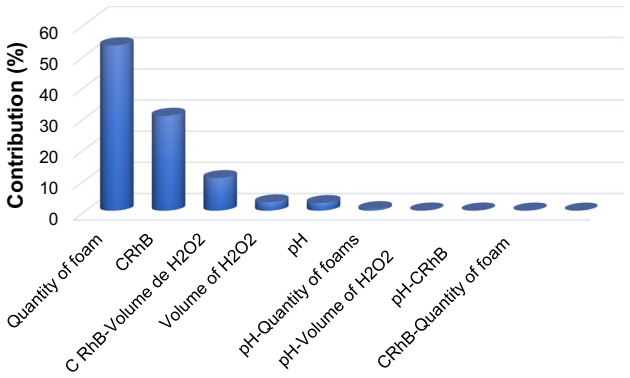

Fig. 4 Graphical Pareto analysis of effect of pH, concentration of RhB, volume of H_2O_2 and number of foam samples on the discoloration efficiency

capable of activating it and generating ·OH and $O_2^{\cdot -}$ radicals. Furthermore, a large number of adsorbed RhB molecules would inhibit the reaction between RhB molecules and ·OH radicals as a result of a lower chance of any direct interaction between them (Ammari et al. 2015; Goyal and Kishore 2017).

Among the interaction between two factors, only X_2X_3 showed a high coefficient ($b_{23} = 3.92$) and also a positive effect on the discoloration rate. The interaction is shown in Fig. 5, and the corner at the top represents the combination of the lower and the higher levels of both factors RhB concentration (X_2) and peroxide volume (X_3).

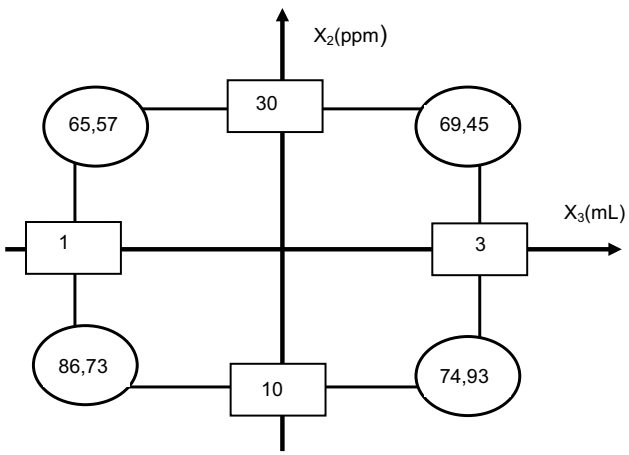

Fig. 5 Interaction between initial concentration of RhB (X_2) and hydrogen peroxide volume (X_3)

Table 5 ANOVA results for full factorial design

Source	Sum of square	Degree of freedom	Mean square	Rapport	Pr > *F*
Regression	2.32738E+0003	10	2.32738E+0002	55.4654	0.0173***
Residual	2.09805E+0001	5	4.19610E+0000		
Total	2.34836E+0003	15			

** < 1%, *** < 0.1%

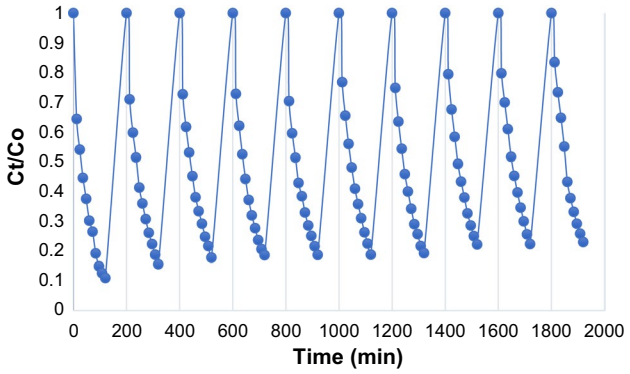

Fig. 6 Kinetics of RhB discoloration for ten solutions treated with TiO_2/β-SiC foam

Table 6 Apparent kinetics (K_{ap}), coefficient of correlation (R^2) and yield (Y%) of ten tests

Number of tests	K_{ap} (10^{-2} min^{-1})	R^2	Y (%)
1	1.94	0.906	90.90
2	1.60	0.968	88.70
3	1.48	0.964	86.50
4	1.51	0.960	87.00
5	1.48	0.934	86.50
6	1.42	0.985	84.20
7	1.45	0.971	85.30
8	1.32	0.981	84.90
9	1.27	0.991	84.00
10	1.28	0.991	84.20

When hydrogen peroxide volume was set at the lowest value (1 mL), RhB concentration produced (induced) a negative influence on the removal which rose from 86.73 to 65.57%. On the one hand, when the dose of peroxide was set at the highest level (3 mL), the concentration varied from 79.93 to 69.45%. These results showed that in order to obtain good discoloration, it is necessary to work with a low concentration of dye at a low dose of H_2O_2. Similar trends were observed by Hamidi and Kacem (2017). They showed that the effectiveness for RhB decolorization is influenced by the ratio $[H_2O_2]/[RhB]$. In this study, the optimum ratio was 6.05 when the H_2O_2 concentration was higher. Two reactions were observed in the production of $HO_2^{\cdot}$ ($E_0 = 1.7$ V) which is less oxidizing than ·OH ($E_0 = 2.8$ V) and not favorable for good removal of organic compounds Eq. (6), and a consumption of hydroxyl radicals (Qourzal et al. 2007; Briton et al. 2019) according to the following reactions in Eq. (7):

$$H_2O_2 + \cdot OH \rightarrow H_2O + HO_2^{\cdot} \quad (6)$$

$$HO_2^{\cdot} + \cdot OH \rightarrow H_2O + O_2 \quad (7)$$

Validity of the model

The model is validated if the value of the correlation coefficient R^2 is close to 1 (Fu et al. 2007). R^2 obtained for the model was 0.991, indicating a good agreement between the predicted values and the measured values. The determined F value which was 55.4654 and the low probability value ($Pr > F = 0.000173$) indicated that the full factorial design used in this study was validated by the results (Table 5).

Study aging of foam

For an application, it is important to evaluate how long the foam can be used without any regeneration; for that purpose, ten different aqueous solutions of RhB (5 L) were consecutively treated with the same foams for 20 h (Fig. 6), without any washing and no regeneration. At the end of each test, the reactor was emptied and new solution was put for the following treatment. The apparent kinetic value constants were very close (Table 6), which means, firstly, that there is no loss of TiO_2 particles by washing out and, secondly, that there is no poisoning of the photocatalyst surface by adsorption of the RhB intermediate by-products. At the end of the ten tests, a yield decrease of only 6.7% was observed. TiO_2/β-SiC foam was weighed before and after the 30 tests; only slight loss of weight of 3% per sample was observed. These results indicated that the material presented a good stability.

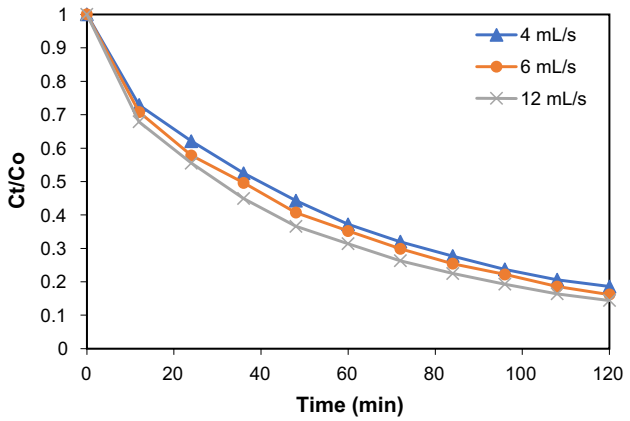

Fig. 7 Influence of flow rate on RhB removal ($C_{RhB} = 10$ ppm)

Effect of the recirculation flow rate on the photocatalytic removal

It is necessary to evaluate the effect of the recirculation flow rate. Figure 7 shows that the increase in flow rate induced a slight increase in discoloration rate from 81.4 to 85.6%. The same observation was done by Kouamé et al. (2012) and Sacco et al. (2018). This increase was due to diffusion between RhB and TiO_2 catalyst which can be explained by the transfer of O_2 an electron scavenger into the liquid phase (Merabet et al. 2009). Thus, it may inhibit the recombination of hole–electron pairs and lead to the oxidation of RhB dye.

Conclusion

A full factorial design (2^4 test) was used to evaluate the effect of pH, dye concentration, volume of H_2O_2 and number of TiO_2 β-sic foam samples on the photocatalytic removal of RhB. The Pareto analysis of the model terms showed that the photocatalytic process was highly influenced by the number of foam samples (53.01%) and the concentration of Rhodamine (30.49%). only the interaction between RhB concentration and volume of H_2O_2 has an influence on the removal rate (10.86%).

Analysis of variance showed the high coefficient of determination values ($R^2 = 0.991$), thus ensuring a satisfactory adjustment of the first-order regression model with the experimental data. Analyses of the coefficients show that initial concentration of RhB and volume of H_2O_2 had a negative effect on the discoloration. However, quantity of TiO_2/β-SiC foam and pH had a positive effect.

The study of aging of the foam had shown a good stability of the material, with a loss of only 3% of TiO_2 after 30 successive tests. Furthermore, it is important to notice that the increase in the recirculation flow rate results in a slight increase in RhB discoloration rate which goes from 81.4 to 85.6%.

Funding This work has not received any funds.

Compliance with ethical standards

Conflict of interest The authors declare that they have no conflict of interest.

Ethical approval The authors certify that article is original work that has not been published elsewhere and approve the submission to Applied Water Science.

Informed consent All authors have endorsed the publication of this research.

References

Aliabadi M, Sagharigar T (2011) Photocatalytic removal of Rhodamine B from aqueous solutions using TiO_2 nanocatalyst. J Appl Environ Biol Sci 1:620–626

Al-Kahtani AA (2016) Photocatalytic degradation of Rhodamine B dye in wastewater using gelatin/CuS/PVA nanocomposites under solar light irradiation. J Biomater Nanobiotechnol 08:66. https://doi.org/10.4236/jbnb.2017.81005

Ammari Y, Elatmani K, Qourzal S et al (2015) Etude cinétique de la dégradation photocatalytique du colorant bleu de méthylène en présence de dioxyde de titane (TiO_2), en suspension aqueuse (Kinetic study of the photocatalytic degradation of methylene blue dye in the presence of titanium dioxide (TiO_2), in aqueous suspension). J Mater Environ Sci 7:671–678

Ano J, Assémian AS, Yobouet YA et al (2019) Electrochemical removal of phosphate from synthetic effluent: a comparative study between iron and aluminum by using experimental design methodology. Process Saf Environ Prot 129:184–195. https://doi.org/10.1016/j.psep.2019.07.003

Ansari SA, Khan MM, Ansari MO, Cho MH (2016) Nitrogen-doped titanium dioxide (N-doped TiO_2) for visible light photocatalysis. New J Chem 40:3000–3009. https://doi.org/10.1039/C5NJ03478G

Antoniou MG, Dionysiou DD (2007) Application of immobilized titanium dioxide photocatalysts for the degradation of creatinine and phenol, model organic contaminants found in NASA's spacecrafts wastewater streams. Catal Today 124:215–223. https://doi.org/10.1016/j.cattod.2007.03.054

Arenas LT, Lima EC, dos Santos AA et al (2007) Use of statistical design of experiments to evaluate the sorption capacity of

1,4-diazoniabicycle[2.2.2]octane/silica chloride for Cr(VI) adsorption. Colloids Surf A 297:240–248. https://doi.org/10.1016/j.colsurfa.2006.10.050

Asiri AM, Al-Amoudi MS, Al-Talhi TA, Al-Talhi AD (2011) Photodegradation of Rhodamine 6G and phenol red by nanosized TiO_2 under solar irradiation. J Saudi Chem Soc 15:121–128. https://doi.org/10.1016/j.jscs.2010.06.005

Assémian AS, Kouassi KE, Drogui P et al (2018) Removal of a persistent dye in aqueous solutions by electrocoagulation process: modeling and optimization through response surface methodology. Water Air Soil Pollut 229:184. https://doi.org/10.1007/s11270-018-3813-2

Assidjo E, Yao B, Akou E, Ado G (2005) Optimisation of the treatment conditions of cocoa butter in order to reduce non-quality. J Chemom 19:543–548. https://doi.org/10.1002/cem.953

Bouyakoub A, Kacha S, Ouhib R et al (2010) Traitement combiné d'un effluent textile contenant des colorants réactifs par coagulation-floculation et électroflottation. Rseau 23:89–103. https://doi.org/10.7202/038927ar

Bouyarmane H (2014) Etude des processus d'adsorption et de photodégradation des polluants organiques supportés sur les composites TiO_2-Apatite. Thèse de Doctorat, Mohammed V–AGDAL

Brasil JL, Martins LC, Ev RR et al (2005) Factorial design for optimization of flow-injection preconcentration procedure for copper(II) determination in natural waters, using 2-aminomethylpyridine grafted silica gel as adsorbent and spectrophotometric detection. Int J Environ Anal Chem 85:475–491. https://doi.org/10.1080/03067310500117350

Briton BGH, Duclaux L, Richardson Y et al (2018) Optimization of total organic carbon removal of a real dyeing wastewater by heterogeneous Fenton using response surface methodology. Desalin Water Treat 136:186–198

Briton BGH, Duclaux L, Richardson Y et al (2019) Effectiveness of the dispersion of iron nanoparticles within micropores and mesopores of activated carbon for Rhodamine B removal in wastewater by the heterogeneous Fenton process. Appl Water Sci 9:166. https://doi.org/10.1007/s13201-019-1047-0

Crişan M, Mardare D, Ianculescu A et al (2018) Iron doped TiO_2 films and their photoactivity in nitrobenzene removal from water. Appl Surf Sci 455:201–215. https://doi.org/10.1016/j.apsusc.2018.05.124

Elhalil A, Tounsadi H, Elmoubarki R et al (2016) Factorial experimental design for the optimization of catalytic degradation of malachite green dye in aqueous solution by Fenton process. Water Resour Ind 15:41–48. https://doi.org/10.1016/j.wri.2016.07.002

Fu JF, Zhao YQ, Wu Q (2007) Optimising photoelectrocatalytic oxidation of fulvic acid using response surface methodology. J Hazard Mater 144:499–505. https://doi.org/10.1016/j.jhazmat.2006.10.071

García-Gómez C, Drogui P, Zaviska F et al (2014) Experimental design methodology applied to electrochemical oxidation of carbamazepine using Ti/PbO_2 and Ti/BDD electrodes. J Electroanal Chem 732:1–10. https://doi.org/10.1016/j.jelechem.2014.08.032

Goyal R, Kishore D (2017) Investigation of photocatalytic degradation of Rhodamine B by using nanosized TiO_2. Int J Sci Res Manag 1(5):6006–6013. https://doi.org/10.18535/ijsrm/v5i7.25

Hafizah N, Sopyan I (2015) Cement bonded sol-gel TiO_2 powder photocatalysis for phenol removal. Appl Mech Mater. https://doi.org/10.4028/www.scientific.net/AMM.776.271

Hamidi N, Kacem M (2017) Dégradation photocatalytique de la Rhodamine B en milieu hétérogène. Université Abou Bekr Belkaid, Tlemcem

Han G, Liang C-Z, Chung T-S et al (2016) Combination of forward osmosis (FO) process with coagulation/flocculation (CF) for potential treatment of textile wastewater. Water Res 91:361–370. https://doi.org/10.1016/j.watres.2016.01.031

Hariprasad N, Anju SG, Yesodharan EP (2013) Sunlight induced removal of Rhodamine B from water through semiconductor photocatalysis: effects of adsorption, reaction conditions and additives. Res J Mater Sci 1:9–17

Joshi M, Bansal R, Purwar R (2004) Colour removal from textile effluents. IJFTR 29:239–259

Kouamé N, Robert D, Keller V et al (2012) TiO_2/SiC foam-structured photoreactor for continuous waste water treatment. Environ Sci Pollut Res Int 19:3727–3734. https://doi.org/10.1007/s11356-011-0719-6

M'Bra IC, García-Muñoz P, Drogui P et al (2019) Heterogeneous photodegradation of Pyrimethanil and its commercial formulation with TiO_2 immobilized on SiC foams. J Photochem Photobiol A 368:1–6. https://doi.org/10.1016/j.jphotochem.2018.09.007

Mansour H, Boughzala O, Dridi D et al (2011) Les colorants textiles sources de contamination de l'eau : CRIBLAGE de la toxicité et des méthodes de traitement. Rseau 24:209–238. https://doi.org/10.7202/1006453ar

Marien C (2017) synthèse, caractérisation et réactivité de matériaux nanostructurés en TiO_2 pour la dégradation photo(électro)catalytique du paraquat. Thèse de Doctorat, Université du Quebec

Martínez-Huitle CA, Brillas E (2009) Decontamination of wastewaters containing synthetic organic dyes by electrochemical methods: a general review. Appl Catal B 87:105–145. https://doi.org/10.1016/j.apcatb.2008.09.017

Merabet S, Bouzaza A, Wolbert D (2009) Photocatalytic degradation of indole in a circulating upflow reactor by UV/TiO_2 process–influence of some operating parameters. J Hazard Mater 166:1244–1249. https://doi.org/10.1016/j.jhazmat.2008.12.047

Montgomery DC (1997) Design and analysis of experiments. Wiley, New York

Papić S, Koprivanac N, Lončarić Božić A, Meteš A (2004) Removal of some reactive dyes from synthetic wastewater by combined Al(III) coagulation/carbon adsorption process. Dyes Pigm 62:291–298. https://doi.org/10.1016/S0143-7208(03)00148-7

Qourzal S, Tamimi M, Assabbane A, Ait-Ichou Y (2007) Influence de certains ions inorganiques, de l'éthanol et du peroxyde d'hydrogène sur la photominéralisation du b-naphtol en présence de TiO_2. C R Chim 10:1187–1194

Sacco O, Vaiano V, Rizzo L, Sannino D (2018) Photocatalytic activity of a visible light active structured photocatalyst developed for municipal wastewater treatment. J Clean Prod 175:38–49. https://doi.org/10.1016/j.jclepro.2017.11.088

Sanzone G, Zimbone M, Cacciato G et al (2018) Ag/TiO_2 nanocomposite for visible light-driven photocatalysis. Superlattices Microstruct 123:394–402. https://doi.org/10.1016/j.spmi.2018.09.028

Sattar M, Hayeeye F, Chinpa W, Sirichote O (2017) Preparation and characterization of poly (lactic acid)/activated carbon composite bead via phase inversion method and its use as adsorbent for Rhodamine B in aqueous solution. J Environ Chem Eng 5:3780–3791. https://doi.org/10.1016/j.jece.2017.07.007

Seck EI, Doña-Rodríguez JM, Fernández-Rodríguez C et al (2012) Photocatalytic removal of 2,4-dichlorophenoxyacetic acid by using sol–gel synthesized nanocrystalline and commercial TiO_2: operational parameters optimization and toxicity studies. Appl Catal B 125:28–34. https://doi.org/10.1016/j.apcatb.2012.05.028

Spasiano D, Marotta R, Malato S et al (2015) Solar photocatalysis: materials, reactors, some commercial, and pre-industrialized applications. A comprehensive approach. Appl Catal B 170–171:90–123. https://doi.org/10.1016/j.apcatb.2014.12.050

Telegang CC (2017) Elaboration de matériaux composites bifonctionnels charbon actif-TiO_2 à partir des ressources végétales tropicales pour des applications de traitement de l'eau par voie solaire. Thèse, Université de Perpinan Via Domitia

Verma AK, Dash RR, Bhunia P (2012) A review on chemical coagulation/flocculation technologies for removal of colour from

textile wastewaters. J Environ Manag 93:154–168. https://doi.org/10.1016/j.jenvman.2011.09.012

Viet PV, Sang TT, Hien NQ et al (2018) Synthesis of a silver/TiO_2 nanotube nanocomposite by gamma irradiation for enhanced photocatalytic activity under sunlight. Nucl Instrum Methods Phys Res Sect B 429:14–18. https://doi.org/10.1016/j.nimb.2018.05.023

Wu J-M, Zhang T-W (2004) Photodegradation of Rhodamine B in water assisted by titania films prepared through a novel procedure. J Photochem Photobiol A 162:171–177. https://doi.org/10.1016/S1010-6030(03)00345-9

Yang H, Yang J (2018) Photocatalytic degradation of rhodamine B catalyzed by TiO_2 films on a capillary column. RSC Adv 8:11921–11929. https://doi.org/10.1039/C8RA00471D